Search for Randall-Sundrum gravitons in the dielectron and diphoton final states with 5.4 fb^{-1} of data from p$\bar{\text{p}}$ collisions at $\sqrt{s} = 1.96$ TeV

V.M. Abazov[36], B. Abbott[74], M. Abolins[63], B.S. Acharya[29], M. Adams[49], T. Adams[47], E. Aguilo[6], G.D. Alexeev[36], G. Alkhazov[40], A. Alton[62,a], G. Alverson[61], G.A. Alves[2], L.S. Ancu[35], M. Aoki[48], Y. Arnoud[14], M. Arov[58], A. Askew[47], B. Åsman[41], O. Atramentov[66], C. Avila[8], J. BackusMayes[81], F. Badaud[13], L. Bagby[48], B. Baldin[48], D.V. Bandurin[47], S. Banerjee[29], E. Barberis[61], A.-F. Barfuss[15], P. Baringer[56], J. Barreto[2], J.F. Bartlett[48], U. Bassler[18], S. Beale[6], A. Bean[56], M. Begalli[3], M. Begel[72], C. Belanger-Champagne[41], L. Bellantoni[48], J.A. Benitez[63], S.B. Beri[27], G. Bernardi[17], R. Bernhard[22], I. Bertram[42], M. Besançon[18], R. Beuselinck[43], V.A. Bezzubov[39], P.C. Bhat[48], V. Bhatnagar[27], G. Blazey[50], S. Blessing[47], K. Bloom[65], A. Boehnlein[48], D. Boline[71], T.A. Bolton[57], E.E. Boos[38], G. Borissov[42], T. Bose[60], A. Brandt[77], R. Brock[63], G. Brooijmans[69], A. Bross[48], D. Brown[19], X.B. Bu[7], D. Buchholz[51], M. Buehler[80], V. Buescher[24], V. Bunichev[38], S. Burdin[42,b], T.H. Burnett[81], C.P. Buszello[43], P. Calfayan[25], B. Calpas[15], S. Calvet[16], E. Camacho-Pérez[33], J. Cammin[70], M.A. Carrasco-Lizarraga[33], E. Carrera[47], B.C.K. Casey[48], H. Castilla-Valdez[33], S. Chakrabarti[71], D. Chakraborty[50], K.M. Chan[54], A. Chandra[79], G. Chen[56], S. Chevalier-Théry[18], D.K. Cho[76], S.W. Cho[31], S. Choi[32], B. Choudhary[28], T. Christoudias[43], S. Cihangir[48], D. Claes[65], J. Clutter[56], M.S. Cooke[69], M. Cooke[48], W.E. Cooper[48], M. Corcoran[79], F. Couderc[18], M.-C. Cousinou[15], A. Croc[18], D. Cutts[76], M. Ćwiok[30], A. Das[45], G. Davies[43], K. De[77], S.J. de Jong[35], E. De La Cruz-Burelo[33], K. DeVaughan[65], F. Déliot[18], M. Demarteau[48], R. Demina[70], D. Denisov[48], S.P. Denisov[39], S. Desai[48], H.T. Diehl[48], M. Diesburg[48], A. Dominguez[65], T. Dorland[81], A. Dubey[28], L.V. Dudko[38], D. Duggan[66], A. Duperrin[15], S. Dutt[27], A. Dyshkant[50], M. Eads[65], D. Edmunds[63], J. Ellison[46], V.D. Elvira[48], Y. Enari[17], S. Eno[59], H. Evans[52], A. Evdokimov[72], V.N. Evdokimov[39], G. Facini[61], A.V. Ferapontov[76], T. Ferbel[59,70], F. Fiedler[24], F. Filthaut[35], W. Fisher[63], H.E. Fisk[48], M. Fortner[50], H. Fox[42], S. Fuess[48], T. Gadfort[72], A. Garcia-Bellido[70], V. Gavrilov[37], P. Gay[13], W. Geist[19], W. Geng[15,63], D. Gerbaudo[67], C.E. Gerber[49], Y. Gershtein[66], D. Gillberg[6], G. Ginther[48,70], G. Golovanov[36], A. Goussiou[81], P.D. Grannis[71], S. Greder[19], H. Greenlee[48], Z.D. Greenwood[58], E.M. Gregores[4], G. Grenier[20], Ph. Gris[13], J.-F. Grivaz[16], A. Grohsjean[18], S. Grünendahl[48], M.W. Grünewald[30], F. Guo[71], J. Guo[71], G. Gutierrez[48], P. Gutierrez[74], A. Haas[69,c], P. Haefner[25], S. Hagopian[47], J. Haley[61], I. Hall[63], L. Han[7], K. Harder[44], A. Harel[70], J.M. Hauptman[55], J. Hays[43], T. Hebbeker[21], D. Hedin[50], A.P. Heinson[46], U. Heintz[76], C. Hensel[23], I. Heredia-De La Cruz[33], K. Herner[62], G. Hesketh[61], M.D. Hildreth[54], R. Hirosky[80], T. Hoang[47], J.D. Hobbs[71], B. Hoeneisen[12], M. Hohlfeld[24], S. Hossain[74], P. Houben[34], Y. Hu[71], Z. Hubacek[10], N. Huske[17], V. Hynek[10], I. Iashvili[68], R. Illingworth[48], A.S. Ito[48], S. Jabeen[76], M. Jaffré[16], S. Jain[68], D. Jamin[15], R. Jesik[43], K. Johns[45], C. Johnson[69], M. Johnson[48], D. Johnston[65], A. Jonckheere[48], P. Jonsson[43], A. Juste[48,d], K. Kaadze[57], E. Kajfasz[15], D. Karmanov[38], P.A. Kasper[48], I. Katsanos[65], R. Kehoe[78], S. Kermiche[15], N. Khalatyan[48], A. Khanov[75], A. Kharchilava[68], Y.N. Kharzheev[36], D. Khatidze[76], M.H. Kirby[51], M. Kirsch[21], J.M. Kohli[27], A.V. Kozelov[39], J. Kraus[63], A. Kumar[68], A. Kupco[11], T. Kurča[20], V.A. Kuzmin[38], J. Kvita[9], S. Lammers[52], G. Landsberg[76], P. Lebrun[20], H.S. Lee[31], W.M. Lee[48], J. Lellouch[17], L. Li[46], Q.Z. Li[48], S.M. Lietti[5], J.K. Lim[31], D. Lincoln[48], J. Linnemann[63], V.V. Lipaev[39], R. Lipton[48], Y. Liu[7], Z. Liu[6], A. Lobodenko[40], M. Lokajicek[11], P. Love[42], H.J. Lubatti[81], R. Luna-Garcia[33,e], A.L. Lyon[48], A.K.A. Maciel[2], D. Mackin[79], R. Madar[18], R. Magaña-Villalba[33], P.K. Mal[45], S. Malik[65], V.L. Malyshev[36], Y. Maravin[57], J. Martínez-Ortega[33], R. McCarthy[71], C.L. McGivern[56], M.M. Meijer[35], A. Melnitchouk[64], D. Menezes[50], P.G. Mercadante[4], M. Merkin[38], A. Meyer[21], J. Meyer[23], N.K. Mondal[29], T. Moulik[56], G.S. Muanza[15], M. Mulhearn[80], E. Nagy[15], M. Naimuddin[28], M. Narain[76], R. Nayyar[28], H.A. Neal[62], J.P. Negret[8], P. Neustroev[40], H. Nilsen[22], S.F. Novaes[5], T. Nunnemann[25], G. Obrant[40], D. Onoprienko[57], J. Orduna[33], N. Osman[43], J. Osta[54], G.J. Otero y Garzón[1], M. Owen[44], M. Padilla[46], M. Pangilinan[76], N. Parashar[53], V. Parihar[76], S.-J. Park[23], S.K. Park[31], J. Parsons[69], R. Partridge[76,c], N. Parua[52], A. Patwa[72], B. Penning[48], M. Perfilov[38], K. Peters[44], Y. Peters[44], G. Petrillo[70], P. Pétroff[16], R. Piegaia[1], J. Piper[63], M.-A. Pleier[72], P.L.M. Podesta-Lerma[33,f], V.M. Podstavkov[48], M.-E. Pol[2], P. Polozov[37], A.V. Popov[39], M. Prewitt[79], D. Price[52], S. Protopopescu[72], J. Qian[62], A. Quadt[23], B. Quinn[64], M.S. Rangel[16], K. Ranjan[28], P.N. Ratoff[42], I. Razumov[39], P. Renkel[78], P. Rich[44], M. Rijssenbeek[71], I. Ripp-Baudot[19], F. Rizatdinova[75], M. Rominsky[48], C. Royon[18], P. Rubinov[48], R. Ruchti[54], G. Safronov[37], G. Sajot[14], A. Sánchez-Hernández[33], M.P. Sanders[25], B. Sanghi[48], G. Savage[48], L. Sawyer[58], T. Scanlon[43], D. Schaile[25], R.D. Schamberger[71], Y. Scheglov[40], H. Schellman[51],

T. Schliephake[26], S. Schlobohm[81], C. Schwanenberger[44], R. Schwienhorst[63], J. Sekaric[56], H. Severini[74],
E. Shabalina[23], V. Shary[18], A.A. Shchukin[39], R.K. Shivpuri[28], V. Simak[10], V. Sirotenko[48], P. Skubic[74],
P. Slattery[70], D. Smirnov[54], G.R. Snow[65], J. Snow[73], S. Snyder[72], S. Söldner-Rembold[44], L. Sonnenschein[21],
A. Sopczak[42], M. Sosebee[77], K. Soustruznik[9], B. Spurlock[77], J. Stark[14], V. Stolin[37], D.A. Stoyanova[39],
M.A. Strang[68], E. Strauss[71], M. Strauss[74], R. Ströhmer[25], D. Strom[49], L. Stutte[48], P. Svoisky[35], M. Takahashi[44],
A. Tanasijczuk[1], W. Taylor[6], B. Tiller[25], M. Titov[18], V.V. Tokmenin[36], D. Tsybychev[71], B. Tuchming[18], C. Tully[67],
P.M. Tuts[69], R. Unalan[63], L. Uvarov[40], S. Uvarov[40], S. Uzunyan[50], R. Van Kooten[52], W.M. van Leeuwen[34],
N. Varelas[49], E.W. Varnes[45], I.A. Vasilyev[39], P. Verdier[20], L.S. Vertogradov[36], M. Verzocchi[48], M. Vesterinen[44],
D. Vilanova[18], P. Vint[43], P. Vokac[10], H.D. Wahl[47], M.H.L.S. Wang[70], J. Warchol[54], G. Watts[81], M. Wayne[54],
G. Weber[24], M. Weber[48,g], M. Wetstein[59], A. White[77], D. Wicke[24], M.R.J. Williams[42], G.W. Wilson[56],
S.J. Wimpenny[46], M. Wobisch[58], D.R. Wood[61], T.R. Wyatt[44], Y. Xie[48], C. Xu[62], S. Yacoob[51], R. Yamada[48],
W.-C. Yang[44], T. Yasuda[48], Y.A. Yatsunenko[36], Z. Ye[48], H. Yin[7], K. Yip[72], H.D. Yoo[76], S.W. Youn[48], J. Yu[77],
S. Zelitch[80], T. Zhao[81], B. Zhou[62], N. Zhou[69], J. Zhu[71], M. Zielinski[70], D. Zieminska[52], and L. Zivkovic[69]

(The DØ Collaboration)

[1] Universidad de Buenos Aires, Buenos Aires, Argentina
[2] LAFEX, Centro Brasileiro de Pesquisas Físicas, Rio de Janeiro, Brazil
[3] Universidade do Estado do Rio de Janeiro, Rio de Janeiro, Brazil
[4] Universidade Federal do ABC, Santo André, Brazil
[5] Instituto de Física Teórica, Universidade Estadual Paulista, São Paulo, Brazil
[6] Simon Fraser University, Burnaby, British Columbia,
Canada; and York University, Toronto, Ontario, Canada
[7] University of Science and Technology of China, Hefei, People's Republic of China
[8] Universidad de los Andes, Bogotá, Colombia
[9] Charles University, Faculty of Mathematics and Physics,
Center for Particle Physics, Prague, Czech Republic
[10] Czech Technical University in Prague, Prague, Czech Republic
[11] Center for Particle Physics, Institute of Physics,
Academy of Sciences of the Czech Republic, Prague, Czech Republic
[12] Universidad San Francisco de Quito, Quito, Ecuador
[13] LPC, Université Blaise Pascal, CNRS/IN2P3, Clermont, France
[14] LPSC, Université Joseph Fourier Grenoble 1, CNRS/IN2P3,
Institut National Polytechnique de Grenoble, Grenoble, France
[15] CPPM, Aix-Marseille Université, CNRS/IN2P3, Marseille, France
[16] LAL, Université Paris-Sud, IN2P3/CNRS, Orsay, France
[17] LPNHE, Universités Paris VI and VII, CNRS/IN2P3, Paris, France
[18] CEA, Irfu, SPP, Saclay, France
[19] IPHC, Université de Strasbourg, CNRS/IN2P3, Strasbourg, France
[20] IPNL, Université Lyon 1, CNRS/IN2P3, Villeurbanne, France and Université de Lyon, Lyon, France
[21] III. Physikalisches Institut A, RWTH Aachen University, Aachen, Germany
[22] Physikalisches Institut, Universität Freiburg, Freiburg, Germany
[23] II. Physikalisches Institut, Georg-August-Universität Göttingen, Göttingen, Germany
[24] Institut für Physik, Universität Mainz, Mainz, Germany
[25] Ludwig-Maximilians-Universität München, München, Germany
[26] Fachbereich Physik, University of Wuppertal, Wuppertal, Germany
[27] Panjab University, Chandigarh, India
[28] Delhi University, Delhi, India
[29] Tata Institute of Fundamental Research, Mumbai, India
[30] University College Dublin, Dublin, Ireland
[31] Korea Detector Laboratory, Korea University, Seoul, Korea
[32] SungKyunKwan University, Suwon, Korea
[33] CINVESTAV, Mexico City, Mexico
[34] FOM-Institute NIKHEF and University of Amsterdam/NIKHEF, Amsterdam, The Netherlands
[35] Radboud University Nijmegen/NIKHEF, Nijmegen, The Netherlands
[36] Joint Institute for Nuclear Research, Dubna, Russia
[37] Institute for Theoretical and Experimental Physics, Moscow, Russia
[38] Moscow State University, Moscow, Russia
[39] Institute for High Energy Physics, Protvino, Russia
[40] Petersburg Nuclear Physics Institute, St. Petersburg, Russia
[41] Stockholm University, Stockholm, Sweden, and Uppsala University, Uppsala, Sweden

[42]*Lancaster University, Lancaster LA1 4YB, United Kingdom*
[43]*Imperial College London, London SW7 2AZ, United Kingdom*
[44]*The University of Manchester, Manchester M13 9PL, United Kingdom*
[45]*University of Arizona, Tucson, Arizona 85721, USA*
[46]*University of California Riverside, Riverside, California 92521, USA*
[47]*Florida State University, Tallahassee, Florida 32306, USA*
[48]*Fermi National Accelerator Laboratory, Batavia, Illinois 60510, USA*
[49]*University of Illinois at Chicago, Chicago, Illinois 60607, USA*
[50]*Northern Illinois University, DeKalb, Illinois 60115, USA*
[51]*Northwestern University, Evanston, Illinois 60208, USA*
[52]*Indiana University, Bloomington, Indiana 47405, USA*
[53]*Purdue University Calumet, Hammond, Indiana 46323, USA*
[54]*University of Notre Dame, Notre Dame, Indiana 46556, USA*
[55]*Iowa State University, Ames, Iowa 50011, USA*
[56]*University of Kansas, Lawrence, Kansas 66045, USA*
[57]*Kansas State University, Manhattan, Kansas 66506, USA*
[58]*Louisiana Tech University, Ruston, Louisiana 71272, USA*
[59]*University of Maryland, College Park, Maryland 20742, USA*
[60]*Boston University, Boston, Massachusetts 02215, USA*
[61]*Northeastern University, Boston, Massachusetts 02115, USA*
[62]*University of Michigan, Ann Arbor, Michigan 48109, USA*
[63]*Michigan State University, East Lansing, Michigan 48824, USA*
[64]*University of Mississippi, University, Mississippi 38677, USA*
[65]*University of Nebraska, Lincoln, Nebraska 68588, USA*
[66]*Rutgers University, Piscataway, New Jersey 08855, USA*
[67]*Princeton University, Princeton, New Jersey 08544, USA*
[68]*State University of New York, Buffalo, New York 14260, USA*
[69]*Columbia University, New York, New York 10027, USA*
[70]*University of Rochester, Rochester, New York 14627, USA*
[71]*State University of New York, Stony Brook, New York 11794, USA*
[72]*Brookhaven National Laboratory, Upton, New York 11973, USA*
[73]*Langston University, Langston, Oklahoma 73050, USA*
[74]*University of Oklahoma, Norman, Oklahoma 73019, USA*
[75]*Oklahoma State University, Stillwater, Oklahoma 74078, USA*
[76]*Brown University, Providence, Rhode Island 02912, USA*
[77]*University of Texas, Arlington, Texas 76019, USA*
[78]*Southern Methodist University, Dallas, Texas 75275, USA*
[79]*Rice University, Houston, Texas 77005, USA*
[80]*University of Virginia, Charlottesville, Virginia 22901, USA and*
[81]*University of Washington, Seattle, Washington 98195, USA*
(Dated: April 11, 2010)

Using 5.4 fb^{-1} of integrated luminosity from $p\bar{p}$ collisions at $\sqrt{s} = 1.96$ TeV collected by the D0 detector at the Fermilab Tevatron Collider, we search for decays of the lightest Kaluza-Klein mode of the graviton in the Randall-Sundrum model to ee and $\gamma\gamma$. We set 95% C.L. lower limits on the mass of the lightest graviton between 560 GeV and 1050 GeV for values of the coupling $k/\overline{M}_{\mathrm{Pl}}$ between 0.01 and 0.1.

The large disparity between the scale of quantum gravity, i.e. the Planck scale, $M_{\mathrm{Pl}} \approx 10^{16}$ TeV, and the electroweak scale, of the order of 1 TeV, is known in the standard model (SM) as the hierarchy problem. In the presence of this hierarchy of scales it is not possible to stabilize the Higgs boson mass at the low values required by experimental data, unless by using an unlikely large amount of fine-tuning.

In the Randall-Sundrum (RS) model [1], the existence of a fifth dimension with a warped spacetime metric is proposed, bounded by two three-dimensional branes. The SM fields are localized on one brane, while gravity originates on the other. With this configuration, the hierarchy problem can be resolved by placing the fundamental scale of gravity near the weak scale, and the apparent weakness of gravity arises from the small overlap of the graviton wavefunction with the SM fields. TeV scales are naturally generated from the Planck scale due to a geometrical exponential factor (the "warp factor"), $\Lambda_\pi = \overline{M}_{\mathrm{Pl}}\exp(-k\pi r_c)$, if $kr_c \approx 12$, where $\overline{M}_{\mathrm{Pl}} = M_{\mathrm{Pl}}/\sqrt{8\pi}$ is the reduced Planck scale, and k and r_c are the curvature scale and compactification radius of the extra dimension, respectively.

Gravitons are the only particles that propagate in the

fifth dimension, and appear as a Kaluza-Klein series [2] of massive excitations (KK gravitons, G) with mass gaps of the order of 1 TeV and a universal coupling to the SM fields. Phenomenologically, it is convenient to express the two RS parameters k and r_c in terms of two direct observables: the mass of the lightest excitation, M_1, and the dimensionless coupling to the SM fields, $k/\overline{M}_{\rm Pl}$. To address the hierarchy problem without the need for fine-tuning, M_1 should be in the TeV range and $0.01 \leq k/\overline{M}_{\rm Pl} \leq 0.1$ [3]. KK graviton resonances could be produced in high energy particle collisions and would subsequently decay to pairs of SM fermions or bosons.

In this Letter, we report a search for the lightest KK graviton in the ee and $\gamma\gamma$ decay channels with the D0 detector at the Fermilab Tevatron Collider, where protons and antiprotons collide at $\sqrt{s} = 1.96$ TeV. For $k/\overline{M}_{\rm Pl} \leq 0.1$, KK gravitons would appear as narrow resonances in the ee and $\gamma\gamma$ invariant mass spectra, with a natural width much smaller than the resolution of the D0 detector and with a branching fraction for the $\gamma\gamma$ decay mode which is twice that of the decay to ee. Previous D0 searches for KK gravitons have excluded $M_1 < 300$ GeV for $k/\overline{M}_{\rm Pl} = 0.01$ and $M_1 < 900$ GeV for $k/\overline{M}_{\rm Pl} = 0.1$ at the 95% C.L. [4]. CDF has recently excluded $M_1 < 889$ GeV for $k/\overline{M}_{\rm Pl} = 0.1$ at the 95% C.L. [5].

The D0 detector [6, 7] consists of tracking detectors, calorimeters, and a muon spectrometer. The tracking system includes a silicon microstrip tracker (SMT) close to the beam and a central fiber tracker (CFT), both located within a 2 T superconducting solenoidal magnet. The liquid-argon and uranium calorimeters consist of a central section covering pseudorapidities $|\eta| \lesssim 1.1$ and two endcap calorimeters that extend the coverage to $|\eta| \approx 4.2$, where $\eta = -\ln[\tan(\theta/2)]$, and θ is the polar angle with respect to the proton beam direction. The azimuthal angle is denoted by ϕ. The electromagnetic (EM) section of the calorimeters is segmented into four longitudinal layers (EMi, i=1,4) with transverse segmentation of $\Delta\eta \times \Delta\phi = 0.1 \times 0.1$, except for the more finely segmented EM3 section where it is 0.05×0.05. A preshower system (CPS) uses plastic scintillators with different orientations located between the solenoid and the cryostat of the central calorimeter and provides precise measurements of the positions of EM showers. The luminosity is measured using plastic scintillator arrays placed in front of the endcap calorimeters. The data sample was collected between July 2002 and June 2009 using triggers requiring at least two clusters of energy deposits in the EM calorimeter and corresponds to an integrated luminosity of 5.4 ± 0.3 fb^{-1}.

We select events with two EM clusters, each with transverse momentum $p_T > 25$ GeV and $|\eta| < 1.1$, reconstructed in a cone of radius $R = \sqrt{(\Delta\eta)^2 + (\Delta\phi)^2} = 0.4$. The EM clusters are required to have at least 97% of their energy deposited in the EM calorimeter, and to have the calorimeter isolation variable $I = [E_{\rm tot}(0.4) - E_{\rm EM}(0.2)]/E_{\rm EM}(0.2) < 0.07$, where $E_{\rm tot}(R)$ [$E_{\rm EM}(R)$] is the total [EM] energy in a cone of radius R.

Given the different branching fractions for the $\gamma\gamma$ and ee decays of the KK graviton, plus the fact that the two channels have different backgrounds, the analysis treats the two channels separately to optimize the sensitivity. If both EM clusters in an event are spatially matched to tracker activity, either a reconstructed track or a density of hits in the SMT and CFT consistent with that of an electron, the event goes in the ee category. Otherwise, the event is put in the $\gamma\gamma$ category.

In the ee category, the two electrons are not required to have opposite charges to avoid the loss due to charge misidentification, and two additional requirements are placed on each EM cluster: (i) the scalar sum of the p_T of all tracks originating from the primary vertex (PV, see below) in an annulus of $0.05 < R < 0.4$ around the cluster, I_{trk}, be less than 2.5 GeV; (ii) the cluster be consistent with the electron shower shape using a χ^2 test and a neural network discriminant [8]. In the $\gamma\gamma$ category, additional requirements are placed on each EM cluster: (i) $I_{trk} < 2.0$ GeV; (ii) the energy-weighted shower width in the $r - \phi$ plane in EM3 be less than 3.7 cm; (iii) the cluster be consistent with the photon shower shape using a neural network discriminant.

Proper reconstruction of the event kinematics requires correct identification of the PV of the hard collision. For events in the ee category, the PV is chosen from the list of vertex candidates as the one with the least probability of being a vertex from a soft $p\bar{p}$ interaction as estimated from the p_T of associated tracks. For the $\gamma\gamma$ category, we use the EM-CPS pointing capability, which reconstructs the axes of EM showers by fitting straight lines to shower positions measured in the four longitudinal calorimeter layers and the CPS. The EM-CPS pointing spatial resolution is 3.7 ± 0.2 cm along the beam axis. If at least one photon candidate is matched to a CPS cluster [9], the vertex consistent with the EM-CPS pointing position is chosen as the PV. For events with no photon candidate having a CPS match or events with inconsistent EM-CPS pointing positions of the two photon candidates, the PV is chosen as the one with the highest number of associated tracks. The PV is required to lie within 60 cm of the geometrical center of the detector along the beam axis. The data include a total of 203586 events (186596 in the ee category and 16990 in the $\gamma\gamma$ category) that satisfy these selection criteria and with the invariant mass of the two EM clusters $M_{ee/\gamma\gamma} > 60$ GeV.

All Monte Carlo (MC) samples used in this analysis were generated using PYTHIA [10] with CTEQ6L1 [11] parton distribution functions (PDFs), and processed through a GEANT-based [12] simulation of the D0 detector and the same reconstruction software as the data. KK graviton signals in the ee and $\gamma\gamma$ decay channels are simulated over the range of parameters 220 GeV $\leq M_1 \leq$

1050 GeV and $0.01 < k/\overline{M}_{Pl} < 0.1$. The accuracy of the PV association has been studied in KK graviton events, where the PV reconstruction efficiency is $\approx 98\%$, with $\approx 96\%$ ($\approx 93\%$) probability to match the true vertex in the ee ($\gamma\gamma$) channel. The simulated and observed invariant mass spectra are compared in ee and $\gamma\gamma$ categories separately. The dominant irreducible background in the ee final state is due to the Drell-Yan (DY) process, where an ee mass-dependent k-factor [13] is applied to correct the PYTHIA spectrum for next-to-next-to-leading order (NNLO) effects. The dominant irreducible background in the $\gamma\gamma$ final state is SM $\gamma\gamma$ production, where PYTHIA $\gamma\gamma$ events are reweighted to reproduce the $\gamma\gamma$ invariant mass spectrum predicted by the next-to-leading-order calculation of DIPHOX [14]. D0 has measured the SM $\gamma\gamma$ differential cross section with respect to the $\gamma\gamma$ invariant mass and in the range used for this analysis (above 60 GeV) the shape of this distribution from DIPHOX agrees with the data [15]. The leading systematic uncertainty on this background's shape arises from the choices in the scales used in the DIPHOX calculation, and is at the level of 10%. The main instrumental background comes from the misidentification of one or two jets as electrons or photons. The shape of the invariant mass spectrum of this source of events is estimated from data by selecting events with EM clusters that are not consistent with electron or photon showers using the χ^2 test (ee category) or the neural network discriminant ($\gamma\gamma$ category). Other SM backgrounds, due to DY $\tau\tau$, $W+\gamma$, WW, ZZ, WZ, W+jets and $t\bar{t}$ production, are small and are estimated using PYTHIA MC events corrected to account for higher order effects [16–18].

Having obtained the shapes of the invariant mass spectra of the various background sources, the background normalization is determined by fitting the invariant mass spectrum of the data to a superposition of the backgrounds in a low-mass control region (60 GeV $< M_{ee/\gamma\gamma} < 200$ GeV), where KK gravitons have been excluded at the 95% C.L. by previous searches. In the fit, the total number of background events is fixed to the number of events observed in the data, and the contributions from SM $\gamma\gamma$, DY ee, and instrumental background are free parameters, while the other SM backgrounds are normalized to their theoretical cross sections. The fit is performed for the ee and $\gamma\gamma$ categories separately. By varying the criteria to select the instrumental background sample and the fitting range, the uncertainty of the background normalization procedure is estimated at the level of 2% (10%) in the ee ($\gamma\gamma$) category.

Figure 1 shows the measured ee and $\gamma\gamma$ invariant mass spectra from the data, superimposed on the expected backgrounds. The data and predicted background are generally in good agreement. In the region around 450 GeV there is an excess of events in the $\gamma\gamma$ invariant mass spectrum. The probability that this excess is exclusively due to backgrounds' fluctuations is 0.011, i.e.
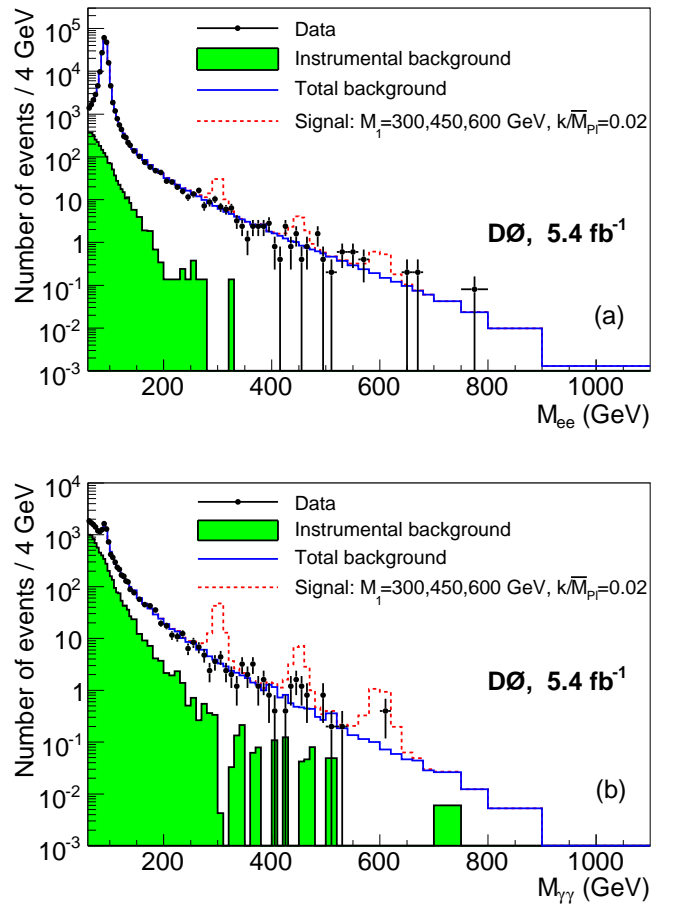

FIG. 1: Invariant mass spectrum from (a) ee and (b) $\gamma\gamma$ data (points). Superimposed are the fitted total background shape from SM processes including instrumental background (open histogram) and the fitted contribution from events with misidentified clusters alone (shaded histogram). The open histogram with dashed line shows the signals expected from KK gravitons with $M_1 = 300$ GeV, 450 GeV, 600 GeV (from left to right) and $k/\overline{M}_{Pl} = 0.02$ on top of the total background. Invariant masses below 200 GeV are taken as the control region.

the background-only hypothesis is disfavored at the 2.30 standard deviations (s.d.) level. This is reduced to 2.16 s.d. when the result from the ee channel is also considered.

In the absence of any significant signal for a heavy narrow resonance, we compute upper limits for the production cross section of KK gravitons times the branching fraction into the ee final state using a Poisson log-likelihood ratio (LLR) test [19]. Invariant mass distributions are utilized in the limit calculation. The ee and $\gamma\gamma$ categories are treated as two independent channels, and then the two separate LLRs are added to obtain a combined exclusion limit assuming the 1:2 ratio of the branching fractions.

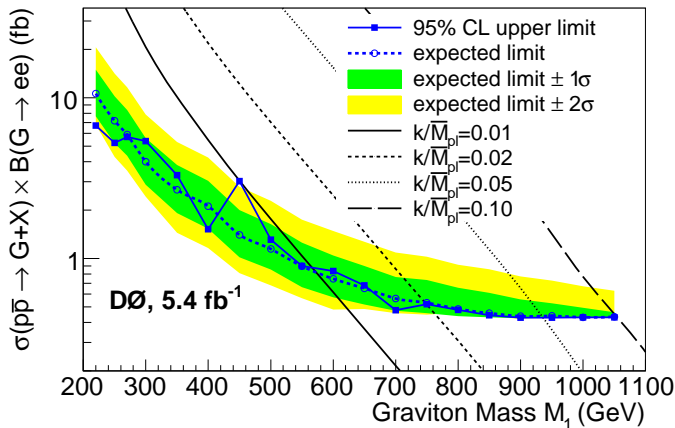Systematic uncertainties on the backgrounds' predic-

FIG. 2: 95% C.L. upper limit on $\sigma(p\bar{p} \to G + X) \times B(G \to ee)$ from 5.4 fb^{-1} of integrated luminosity compared with the expected limit and the theoretical predictions for different couplings $k/\overline{M}_{\mathrm{Pl}}$.

TABLE I: 95% C.L. upper limit on $\sigma(p\bar{p} \to G+X) \times B(G \to ee)$ and coupling $k/\overline{M}_{\mathrm{Pl}}$ from 5.4 fb^{-1} of integrated luminosity.

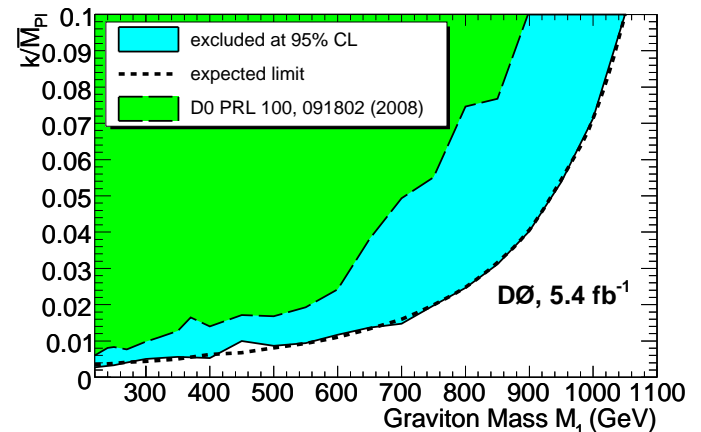| Graviton Mass | $\sigma \times B(G \to ee)$ (fb) | | Coupling $k/\overline{M}_{\mathrm{Pl}}$ | |
GeV	Expected	Observed	Expected	Observed
220	10.62	6.71	0.0034	0.0027
250	7.18	5.23	0.0038	0.0033
270	5.91	5.69	0.0042	0.0041
300	4.00	5.37	0.0044	0.0050
350	2.67	3.30	0.0051	0.0056
400	2.12	1.52	0.0062	0.0053
450	1.40	3.03	0.0068	0.0099
500	1.15	1.31	0.0081	0.0087
550	0.89	0.90	0.0093	0.0094
600	0.75	0.84	0.0111	0.0117
650	0.65	0.68	0.0133	0.0136
700	0.56	0.48	0.0160	0.0147
750	0.53	0.52	0.0199	0.0197
800	0.48	0.48	0.0248	0.0247
850	0.46	0.44	0.0316	0.0312
900	0.44	0.43	0.0406	0.0403
950	0.44	0.43	0.0545	0.0539
1000	0.43	0.43	0.0713	0.0713
1050	0.43	0.43	0.0969	0.0964

FIG. 3: 95% C.L. upper limit on $k/\overline{M}_{\mathrm{Pl}}$ versus the graviton mass M_1 from 5.4 fb^{-1} of integrated luminosity compared with the expected limit and the previously published exclusion contour [4].

tions and on the signal efficiency are considered to calculate limits. These include the integrated luminosity (6.1%), PDFs (0.7% - 6.6% for the acceptance and 9.2% - 16.9% for the graviton production cross section), electron and photon identification efficiency (3.0% per object), EM cluster energy resolution (6%), and trigger efficiency (0.1%). Uncertainties affecting the expected backgrounds arise from electron and photon identification efficiency (3.0% per object), mass dependence of the DY ee NNLO k-factor (5.0%), shape of the SM $\gamma\gamma$ invariant mass spectrum, and background normalization. For the EM energy resolution, the SM $\gamma\gamma$ invariant mass spectrum and the background normalization we consider both the effects on the normalization and on the shape of the invariant mass distribution used in extracting limits. For all other systematic sources we consider only changes to the overall background normalization or signal detection efficiency. Systematic uncertainties are incorporated via convolution of the Poisson probability distributions for signal and background with Gaussian distributions corresponding to the different sources of systematic uncertainty. Correlations in the systematic uncertainties between signal and background in ee and $\gamma\gamma$ categories are taken into account.

The resulting limits on the production cross section times branching fraction into electron-positron pairs of the lightest KK graviton, $\sigma(p\bar{p} \to G + X) \times B(G \to ee)$, are given in Table I and displayed in Fig. 2. As shown in Fig. 3, using the cross section predictions from the Randall-Sundrum model with a k-factor of 1.54 [20], we can express these results as upper limits on the coupling $k/\overline{M}_{\mathrm{Pl}}$ as a function of M_1.

In summary, using 5.4 fb^{-1} of integrated luminosity collected with the D0 detector at the Fermilab Tevatron Collider, we have searched for a heavy narrow res-

onance in the ee and $\gamma\gamma$ invariant mass spectra. The observed spectra agree with predictions from SM background processes. For the Randall-Sundrum model with a warped extra dimension, we set 95% C.L. upper limits on $\sigma(p\bar{p} \to G + X) \times B(G \to ee)$ of the lightest Kaluza-Klein mode of the graviton between 6.7 fb and 0.43 fb for masses between 220 GeV and 1050 GeV at the 95% C.L., which translate into lower limits on the mass M_1 of the lightest Kaluza-Klein excitation of the graviton between 560 GeV and 1050 GeV for couplings of the graviton to the SM fields $0.01 \leq k/\overline{M}_{\mathrm{Pl}} \leq 0.1$. These results repre-

sent the most sensitive limits to date.

[a] Visitor from Augustana College, Sioux Falls, SD, USA.
[b] Visitor from The University of Liverpool, Liverpool, UK.
[c] Visitor from SLAC, Menlo Park, CA, USA.
[d] Visitor from ICREA/IFAE, Barcelona, Spain.
[e] Visitor from Centro de Investigacion en Computacion - IPN, Mexico City, Mexico.
[f] Visitor from ECFM, Universidad Autonoma de Sinaloa, Culiacán, Mexico.
[g] Visitor from Universität Bern, Bern, Switzerland.

[1] L. Randall and R. Sundrum, Phys. Rev. Lett. **83**, 3370 (1999).
[2] *Modern Kaluza − Klein Theories*, edited by T. Appelquist, A. Chodos, and P. G. O. Freund (Addison-Wesley, Reading, MA, 1987).
[3] H. Davoudiasl, J. L. Hewett, and T. G. Rizzo, Phys. Rev. Lett. **84**, 2080 (2000); Phys. Rev. D **63**, 075004 (2001).
[4] D0 Collaboration, V. Abazov *et al.*, Phys. Rev. Lett. **100**, 091802 (2008).
[5] CDF Collaboration, T. Aaltonen *et al.*, Phys. Rev. Lett. **99**, 0171802 (2007).
[6] D0 Collaboration, V. Abazov *et al.*, Nucl. Instrum. Methods Phys. Res. A **565**, 463 (2006).
[7] D0 Collaboration, S. Abachi *et al.*, Nucl. Instrum. Methods Phys. Res. A **338**, 185 (1994).
[8] D0 Collaboration, V. Abazov *et al.*, Phys. Rev. Lett. **102**, 231801 (2009).
[9] D0 Collaboration, V. Abazov *et al.*, Phys. Lett. B **659**, 856 (2008).
[10] T. Sjöstrand *et al.*, Comput. Phys. Commun. **135**, 238 (2001).
[11] J. Pumplin *et al.*, JHEP **0207** 012 (2002); D. Stump *et al.*, JHEP **0310** 046 (2003).
[12] R. Brun and F. Carminati, CERN Program Library Long Writeup W5013, 1993 (unpublished).
[13] R. Hamberg, W. L. van Neerven, and T. Matsuura, Nucl. Phys. **B359**, 343 (1991) [Erratum-ibid. **B644**, 403 (2002)].
[14] T. Binoth *et al.*, Eur. Phys. J **C16**, 311 (2000).
[15] D0 Collaboration, V. Abazov *et al.*, arXiv:1002.4917 [hep-ex] (2010), submitted for publication in Phys. Lett. B.
[16] J. M. Campbell and R. K. Ellis, Phys. Rev. D **60**, 113006 (1999).
[17] U. Baur and E. L. Berger, Phys. Rev. D **41**, 1476 (1990).
[18] N. Kidonakis and R. Vogt, Phys. Rev. D **68**, 114014 (2003); M. Cacciari *et al.*, JHEP **04**, 68 (2004).
[19] W. Fisher, FERMILAB-TM-2386-E (2006).
[20] P. Mathews *et al.*, JHEP **0510**, 031 (2005).